

## Redesigning the Zinc Binding Site of Human Carbonic Anhydrase II: Structure of a His<sub>2</sub>Asp–Zn<sup>2+</sup> Metal Coordination Polyhedron

Laura L. Kiefer,<sup>‡</sup> Joseph A. Ippolito,<sup>†</sup> Carol A. Fierke,<sup>\*‡</sup> and David W. Christianson<sup>\*‡</sup>

Department of Chemistry  
University of Pennsylvania  
Philadelphia, Pennsylvania 19104-6323  
Department of Biochemistry  
Duke University Medical Center, Box 3711  
Durham, North Carolina 27710

Received September 1, 1993

The goal of protein design is to construct a stable protein molecule having predictable structure and function. Although some success toward this end has been reported,<sup>1</sup> the folding problem (i.e., the unknown relationship between primary and tertiary protein structure) hinders the design and construction of *de novo* proteins. Therefore, we currently focus on protein redesign—the rational alteration of selected regions of a stable, preexisting protein scaffolding in order to confer new functional properties upon that scaffolding. Ultimately, the results of protein redesign studies will be applied toward the *de novo* design of proteins with novel functions. Implicit requirements of protein design and redesign experiments are the availabilities of both well-characterized functional properties and high-resolution protein structures determined by X-ray crystallographic methods.

Our current experiments in protein redesign focus on the chemistry and structure of transition-metal binding sites. Previously, the redesign of copper binding sites in copper–zinc superoxide dismutase<sup>2</sup> and blue copper proteins such as azurin<sup>3</sup> yielded metal sites with altered spectroscopic and catalytic properties. Here, the avid zinc binding site of human carbonic anhydrase II (CAII,  $K_d = 4$  pM)<sup>4</sup> is our paradigm. The His<sub>3</sub>–Zn<sup>2+</sup> motif of this metalloenzyme is the target for *de novo* protein (re)design experiments,<sup>1,5–7</sup> which are particularly illuminating when accompanied by high-resolution structural analysis of the

redesigned paradigm.<sup>4,8,9</sup> Here, we report the three-dimensional structure of the His-94→Asp (H94D) variant of CAII, which contains the first successfully-engineered tetrahedral zinc coordination polyhedron of composition His<sub>2</sub>Asp–Zn<sup>2+</sup>. In addition to its resemblance to the His<sub>2</sub>Asp–Zn<sup>2+</sup> site in alkaline phosphatase, the His<sub>2</sub>Asp–Zn<sup>2+</sup> motif engineered into CAII is chemically comparable to the His<sub>2</sub>Glu–Zn<sup>2+</sup> sites found in zinc proteases such as carboxypeptidase A and thermolysin.<sup>10</sup>

The H94D variant of CAII was produced using oligonucleotide-directed mutagenesis of the cloned CAII gene and purified to ≥95% homogeneity by chromatography on DEAE–Sephacel and S-Sepharose resins.<sup>8</sup> The effect of replacement of the histidine zinc ligand with aspartate on metal binding was assessed by measuring a zinc dissociation constant ( $K_d$ ) using equilibrium dialysis.<sup>4,8</sup> The zinc  $K_d = 15 \pm 5$  nM determined for H94D at pH 7 is increased ~10<sup>4</sup>-fold relative to  $K_d = 4 \pm 1$  pM for wild-type CAII at the same pH. However, the zinc affinity is still significantly higher than that of other designed metal binding sites with three protein ligands.<sup>5–7</sup>

Wild-type CAII catalyzes the hydration of CO<sub>2</sub> to HCO<sub>3</sub><sup>-</sup> and a H<sup>+</sup> with a second-order rate constant that approaches the diffusion control limit; CAII will also catalyze the hydrolysis of some esters.<sup>11</sup> These reactions proceed through nucleophilic attack of zinc-bound hydroxide on the carbonyl carbon of the substrate. The p*K*<sub>a</sub> of the zinc-bound water increases from 6.8 in wild-type CAII to ≥9.6 in H94D CAII, as determined by measuring the pH dependence of CAII-catalyzed *p*-nitrophenyl acetate (PNPA) hydrolysis.<sup>11,12</sup> The second-order rate constant for PNPA hydrolysis by H94D decreases ~7-fold relative to wild-type CAII from 2500 to ≥365 M<sup>-1</sup> s<sup>-1</sup>. Steady-state kinetic parameters for CO<sub>2</sub> hydration were measured for H94D in TAPS buffer at pH 8.9<sup>13</sup> and are listed with the wild-type values in parentheses:  $k_{cat} = 8 \pm 4$  (1000) ms<sup>-1</sup>,  $k_{cat}/K_M = 0.11 \pm 0.01$  (100) μM<sup>-1</sup> s<sup>-1</sup>, and  $K_M = 75 \pm 40$  (8) mM. The large decreases in activity for CO<sub>2</sub> hydration reflect both the decreased catalytic efficiency and the increased p*K*<sub>a</sub>.

The structure of H94D CAII was determined by X-ray crystallographic methods, and crystals were prepared as described.<sup>8,9</sup> X-ray data from one of these crystals were collected to a limiting resolution of 2.3 Å on a Siemens multiwire area detector mounted on a Rigaku RU-200 X-ray generator. Raw data frames were processed using BUDDHA,<sup>14</sup> and data reduction was accomplished with PROTEIN.<sup>15,16</sup> The protein model was adjusted to fit electron density maps using the graphics program CHAIN<sup>17</sup> (maps were calculated by routines contained in X-PLOR<sup>18</sup>), and the model was refined with PROLSQ.<sup>19</sup>

(8) (a) Alexander, R. S.; Kiefer, L. L.; Fierke, C. A.; Christianson, D. W. *Biochemistry* 1993, 32, 1510–1518. (b) Kiefer, L. L.; Ippolito, J. A.; Fierke, C. A.; Christianson, D. W., manuscript in preparation.

(9) Ippolito, J. A.; Christianson, D. W. *Biochemistry* 1993, 32, 9901–9905.

(10) (a) Kim, E. E.; Wyckoff, H. W. *J. Mol. Biol.* 1991, 218, 449–464. (b) Rees, D. C.; Lewis, M.; Lipscomb, W. N. *J. Mol. Biol.* 1983, 168, 367–387. (c) Holmes, M. A.; Matthews, B. W. *J. Mol. Biol.* 1982, 160, 623–639.

(11) (a) Pocker, Y.; Sarkanen, S. *Adv. Enzymol.* 1978, 47, 149–274. (b) Silverman, D. F.; Lindskog, S. *Acc. Chem. Res.* 1988, 21, 30–36.

(12) Krebs, J. F.; Ippolito, J. A.; Christianson, D. W.; Fierke, C. A. *J. Biol. Chem.* in press.

(13) Khalifah, R. G. *J. Biol. Chem.* 1971, 246, 2561–2573.

(14) Durbini, R. M.; Burns, R.; Moulai, J.; Metcalf, P.; Freymann, D.; Blum, M.; Anderson, J. E.; Harrison, S. C.; Wiley, D. C. *Science* 1986, 232, 1127–1132.

(15) Steigemann, W. Ph.D. Thesis, Max-Planck-Institut für Biochemie, 8033 Martinsreid bei München, Germany, 1974.

(16) The *R*-factor for scaling and merging the X-ray data from one crystal was 0.086, where  $R = \sum |I_{hi} - \langle I_{hi} \rangle| / \sum \langle I_{hi} \rangle$ ;  $I_{hi}$  = scaled intensity for reflection *h* in data set *i*,  $\langle I_{hi} \rangle$  = average intensity for reflection *h* calculated from replicate data.

(17) Sack, J. S. *J. Mol. Graphics* 1988, 6, 224–225.

(18) Brünger, A. T.; Kuriyan, J.; Karplus, J. *Science* 1987, 235, 458–460.

(19) Hendrickson, W. A. *Methods Enzymol.* 1985, 115, 252–270.

\* Authors to whom correspondence should be addressed.

† University of Pennsylvania. Telephone: (215) 898-5714. FAX: (215) 573-2201.

‡ Duke University Medical Center. Telephone: (919) 684-2557. FAX: (919) 684-5040.

(1) Handel, T. M.; Williams, S. A.; DeGrado, W. F. *Science* 1993, 261, 879–885.

(2) (a) Lu, Y.; Gralla, E. B.; Roe, J. A.; Valentine, J. S. *J. Am. Chem. Soc.* 1992, 114, 3560–3562. (b) Lu, Y.; LaCroix, L. B.; Lowery, M. D.; Solomon, E. I.; Bender, C. J.; Peisach, J.; Roe, J. A.; Gralla, E. B.; Valentine, J. S. *J. Am. Chem. Soc.* 1993, 115, 5907–5918.

(3) (a) Murphy, L. M.; Strange, R. W.; Karlsson, B. G.; Lundberg, L. G.; Pascher, T.; Reinhammer, B.; Hasnain, S. S. *Biochemistry* 1993, 32, 1965–1975. (b) Karlsson, B. G.; Nordling, M.; Pascher, T.; Tsai, L.-C.; Sjölin, L.; Lundberg, L. G. *Protein Eng.* 1991, 4, 343–349. (c) Chang, T. K.; Iverson, S. A.; Rodrigues, C. G.; Kiser, C. N.; Lew, A. Y. C.; Germanas, J. P.; Richards, J. H. *Proc. Natl. Acad. Sci. U.S.A.* 1991, 88, 1325–1329. (d) den Blaauwen, T.; Canters, G. W. *J. Am. Chem. Soc.* 1993, 115, 1121–1129. (e) Romero, A.; Hoihtink, C. W. G.; Nar, H.; Huber, R.; Messerschmidt, A.; Canters, G. W. *J. Mol. Biol.* 1993, 229, 1007–1021.

(4) Kiefer, L. L.; Krebs, J. F.; Paterno, S. A.; Fierke, C. A. *Biochemistry* 1993, 32, 9896–9900.

(5) (a) Iverson, B. L.; Iverson, S. A.; Roberts, V. A.; Getzoff, E. D.; Tainer, J. A.; Benkovic, S. J.; Lerner, R. A. *Science* 1990, 249, 659–662. (b) Roberts, V. A.; Iverson, B. L.; Iverson, S. A.; Benkovic, S. J.; Lerner, R. A.; Getzoff, E. D.; Tainer, J. A. *Proc. Natl. Acad. Sci. U.S.A.* 1990, 87, 6654–6658. (c) Wade, W. S.; Koh, J. S.; Han, N.; Hoekstra, D. M.; Lerner, R. A. *J. Am. Chem. Soc.* 1993, 115, 4449–4456. (d) Pessi, A.; Bianchi, E.; Cramer, A.; Venturini, S.; Tramontano, A.; Sollazzo, M. *Nature* 1993, 362, 367–369.

(6) (a) Ghadiri, M. R.; Choi, C. *J. Am. Chem. Soc.* 1990, 112, 1630–1632. (b) Ruan, F.; Chen, Y.; Hopkins, P. B. *J. Am. Chem. Soc.* 1990, 112, 9403–9404. (c) Suh, S.-S.; Haymore, B. L.; Arnold, F. H. *Protein Eng.* 1991, 4, 301–305.

(7) (a) Handel, T.; DeGrado, W. F. *J. Am. Chem. Soc.* 1990, 112, 6710–6711. (b) Regan, L.; Clarke, N. D. *Biochemistry* 1990, 29, 10878–10883.

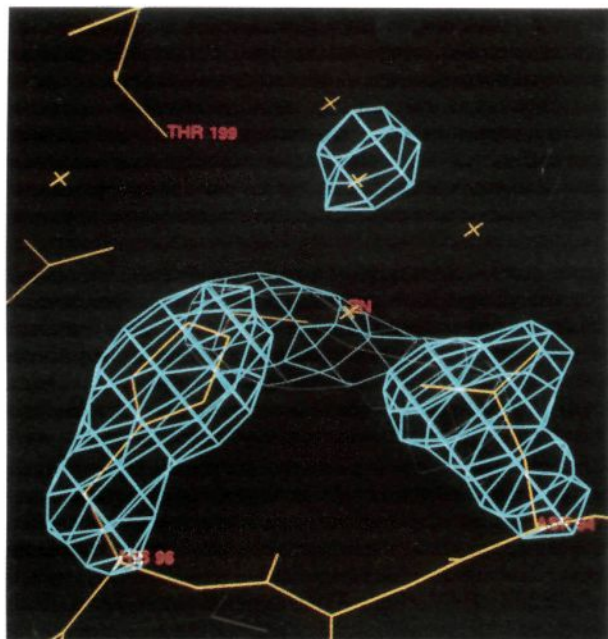


**Figure 1.** Difference electron density map generated with Fourier coefficients  $|F_o| - |F_c|$  and phases calculated from the final H94D CAII model less the side chains of Asp-94, His-96, His-119, and the non-protein zinc ligand. The map is contoured at  $3.5\sigma$ , and refined atomic coordinates are superimposed; Asp-94, His-96, Thr-199, and  $Zn^{2+}$  are indicated.

Refinement converged smoothly to a final crystallographic *R*-factor of 0.170.<sup>20</sup>

The electron density map of Figure 1 reveals tetrahedral zinc coordination by Asp-94, His-96, His-119, and a non-protein ligand. The engineered carboxylate group of Asp-94 coordinates to zinc with *syn*-unidentate stereochemistry ( $O_{\beta 1}-Zn^{2+}$  separation = 2.1 Å), which is consistent with expectations based on analyses of small molecule<sup>21</sup> and protein<sup>22,23</sup> crystal structures. The  $C_{\gamma}-O_{\beta 1}-Zn^{2+}$  angle is  $133^\circ$ , and the interaction is almost precisely within the plane of the carboxylate group. In wild-type CAII, His-94 donates a hydrogen bond to the side-chain carbonyl of Gln-92. The  $O_{\delta 2}$  atom of Asp-94 is within hydrogen-bonding distance (2.9 Å) of Gln-92; additionally,  $O_{\delta 2}$  also forms a strong *syn* hydrogen bond (2.6 Å) with an active-site water molecule, which in turn hydrogen bonds to the non-protein zinc ligand.

Apart from the zinc coordination polyhedron, the structure of H94D CAII does not differ significantly from that of wild-type CAII<sup>24</sup> (root mean square deviation of  $C_{\alpha}$  coordinates = 0.2 Å). The superposition of H94D and wild-type CAII shows that the position of the engineered Asp-94 side chain is isosteric with that of the wild-type His-94 side chain, and the  $\beta$ -sheet superstructure containing Asp-94 is not disrupted. However, because the His $\rightarrow$ Asp substitution is not completely isosteric with respect to

(20)  $R = \sum |F_o| - |F_c| / \sum |F_o|$ ;  $|F_o|$  and  $|F_c|$  are the observed and calculated structure factors, respectively.

(21) Carrell, C. J.; Carrell, H. L.; Erlebacher, J.; Glusker, J. P. *J. Am. Chem. Soc.* **1988**, *110*, 8651–8656.

(22) Christianson, D. W.; Alexander, R. S. *J. Am. Chem. Soc.* **1989**, *111*, 6412–6419.

(23) Chakrabarti, P. *Protein Eng.* **1990**, *4*, 49–56.

(24) Alexander, R. S.; Nair, S. K.; Christianson, D. W. *Biochemistry* **1991**, *30*, 11064–11072.

zinc-coordinating atoms (the  $N_{\epsilon}$  atom of His-94 coordinates to zinc in wild-type CAII, whereas the  $O_{\beta 1}$  of Asp-94 coordinates to zinc in the variant), the zinc ion moves nearly 1 Å toward Asp-94. Consequently, His-96 and His-119 rotate slightly to maintain metal coordination, and the His-96  $N_{\epsilon}-Zn^{2+}$  separation increases from 2.1 to 2.4 Å. These structural changes undoubtedly contribute to decreased protein–zinc affinity. Structural changes in the apoenzyme may also contribute, and these effects incur a net free energy cost of 4.8 kcal mol<sup>-1</sup>.

The electron density map of the H94D CAII active site reveals changes in the binding mode of the non-protein zinc ligand which is modeled and refined satisfactorily as a water molecule, although we cannot exclude the possibility of ammonia or disordered Tris binding.<sup>25</sup> Although Tris does not coordinate to the zinc ion of wild-type CAII, other nitrogen ligands are known to coordinate by displacing the zinc-bound solvent molecule.<sup>26,27</sup>

In H94D CAII, the non-protein zinc ligand forms a weak hydrogen bond with the side chain of Thr-199 ( $O-H$  separation = 3.3 Å); this interaction normally orients the zinc-bound hydroxyl group for substrate attack and maintains the low  $pK_a$  of zinc- $H_2O$ .<sup>12,28,29</sup> Based on a comparison between the properties of T199A<sup>12,29</sup> and H94D CAIIs, we conclude that a majority of the decrease in catalytic efficiency and a portion of the increase in  $pK_a$  arises from a weakened hydrogen bond between Thr-199 and zinc-bound water in H94D CAII. It is likely that the decreased electrostatic stabilization of both the ground-state zinc–hydroxide and the transition state, caused by substitution of a negatively charged aspartate for a neutral histidine ligand, also affects these properties.

In summary, we have successfully replaced a naturally occurring histidine zinc ligand with an aspartate residue in the redesign of the CAII zinc binding site. The properties of H94D CAII demonstrate that: (1) the hydrogen bond network involving zinc-bound solvent is crucial for catalysis; (2) the chemical nature of the protein zinc ligands dictates the  $pK_a$  of zinc-bound solvent with little effect on its reactivity; and (3) the protein structure is sufficiently plastic to allow subtle rearrangements which accommodate metal binding with optimal stereochemistry. Furthermore, this work represents a first step toward conferring new catalytic functions on CAII as well as illuminating structure–function relationships that will facilitate the design of *de novo* metalloproteins with specific catalytic functions.<sup>30,31</sup>

(25) (a) Higaki, J. N.; Haymore, B. L.; Chen, S.; Fletterick, R. J.; Craik, C. S. *Biochemistry* **1990**, *29*, 8582–8586. (b) McGrath, M. E.; Haymore, B. L.; Summers, N. L.; Craik, C. S.; Fletterick, R. J. *Biochemistry* **1993**, *32*, 1914–1919.

(26) Bertini, I.; Luchinat, C.; Scozzafava, A. *J. Am. Chem. Soc.* **1977**, *99*, 581–584.

(27) (a) Bertini, I.; Luchinat, C. *Acc. Chem. Res.* **1983**, *16*, 272–279. (b) Nair, S. K.; Christianson, D. W. *Eur. J. Biochem.* **1993**, *213*, 507–515. (c) Mangani, S.; Liljas, A. *J. Mol. Biol.* **1993**, *232*, 9–14.

(28) Merz, K. M., Jr. *J. Mol. Biol.* **1990**, *214*, 799–802.

(29) (a) Xue, Y.; Liljas, A.; Jonsson, B.-H.; Lindskog, S. *Proteins: Struct., Funct. Genet.* **1993**, *17*, 93–106. (b) Liang, Z.; Xue, Y.; Behravan, G.; Jonsson, B.-H.; Lindskog, S. *Eur. J. Biochem.* **1993**, *211*, 821–827.

(30) Atomic coordinates of H94D CAII have been deposited into the Brookhaven Protein Data Bank with the accession code 1CVC; see: Bernstein, F. C.; Koetzle, T. F.; Williams, G. J. B.; Meyer, E. F.; Brice, M. D.; Rodgers, J. R.; Kennard, O.; Shimanouchi, T.; Tasumi, M. *J. Mol. Biol.* **1977**, *112*, 535–542.

(31) This work was supported by the Office of Naval Research (D.W.C.) and the NIH (Grant GM40602 to C.A.F.). C.A.F. acknowledges an American Heart Association Established Investigatorship and a David and Lucile Packard Foundation Fellowship, and D.W.C. acknowledges an Alfred P. Sloan Research Fellowship and a Camille and Henry Dreyfus Teacher-Scholar Award. J.A.I. is supported in part by NIH Training Grant GM08275.